Extreme Mechanics Letters 55 (2022) 101789

Contents lists available at ScienceDirect

Extreme Mechanics Letters

journal homepage: www.elsevier.com/locate/eml

Wave characteristics of extremal elastic materials

Yu Wei, Gengkai Hu *

School of Aerospace Engineering, Beijing Institute of Technology, Beijing 100081, China

ARTICLE INFO

Article history:
Received 6 February 2022
Received in revised form 12 May 2022
Accepted 12 May 2022
Available online 21 May 2022

Keywords:
Extremal materials
Rank-deficient
Slowness surfaces
Elastic wave

ABSTRACT

The elasticity tensors of extremal materials are rank-deficient, they have inherent easy deformation modes without spending energy. Kinds of materials are classified by the number of vanishing eigenvalues of their elastic matrices, namely from unimode, bimode to pentamode. They may exhibit unprecedented capacity to manipulate waves, as already exemplified by pentamode materials. The peculiar property of these materials on wave propagation lies in reducing the number of slowness surfaces as well as the opening of these surfaces along certain directions determined by easy deformation modes. We demonstrate these wave characteristics according to the classification of extremal materials by analyzing their acoustic tensors. It is shown that the number of slowness surfaces is determined by the number of independent characteristic force vectors provided by the hard modes of the extremal materials on any wave front plane. As a consequence, there is only one slowness surface for pentamode materials, and two for quadramode materials. Trimode materials may have two or three depending whether the three force vectors provided by the materials are coplanar or not. All the other modes definitely have three slowness surfaces. The opening of these surfaces depends on null of these force vectors along certain directions, controlled by the soft deformation modes in these materials. Concrete examples are also given to illustrate these findings. A device of broadband zero-refractive-index for elastic wave is proposed with a trimode material. These works pave the way to design wave devices by exploiting extremal materials.

1. Introduction

The elasticity tensors of stable materials are always required to be positive definite, so that their Christoffel's acoustic tensors are also positive definite [1], i.e., they will produce static and dynamic responses to arbitrary type of external excitation. With the development of elastic metamaterials, some constraints on elasticity tensor have been progressively relaxed, for instance, elastic modulus can turn to negative if resonance is introduced [2–4], or the constraints on major [5,6] and minor [7,8] symmetry of elasticity tensor can be released by allowing external energy exchange, or by careful microstructure design [9]. These extensions equip classical continuum mechanics more power to characterize complex phenomena exhibited by architectured materials.

Extremal materials with rank-deficient elasticity tensor are no longer stable, they are armed with easy deformation modes, i.e., zero energy modes. The *mechanisms* represented by the eigenvector of the zero eigenvalue of elastic matrix allow deformation without any cost of energy. According to Milton and Cherkaev [10,11], these extremal materials were classified by the number of zero eigenvalues of their elastic matrices: if there is one zero-eigenvalue, called unimode (UM) materials, successively bimode (BM), trimode (TM), quadramode (QM), pentamode (PM) if there are five. Since the elasticity tensors of these extremal materials are no longer positive definite, they may exhibit a powerful platform for manipulating waves.

The required mechanism in extremal materials can be approximately realized by flexible microstructure, e.g., replacing a joint by flexible beam in bending [12]. Since the proposition of extremal materials, major efforts are focused on PM lattices, the simplest extremal materials with five zero-eigenvalues of their elastic matrices [10,12–17]. Some studies are conducted to design 2D [10,18–22] or 3D [10,22] UM materials, and more recently QM lattice [23]. The first approximate 3D isotropic solid PM material was fabricated by Kadic et al. [24], the large ratio of tensile modulus over the shear modulus is confirmed experimentally with macroscopic polymer-based samples by a 3D printing technique [25]. The study on PM materials has been further fueled by their potential to realize perfect acoustic cloak [26]. Since only static mechanical property is used without resonance, the devices made of solid extremal materials are intrinsically broadband and are of great value in underwater acoustic wave control. For examples, static "unfeelability" mechanical cloak [27], under water sound cloak [28], polarization tailoring [29,30], seismic wave alleviation [31], SH-wave polarizer [23], negative refractive index [21], low frequency sound insulation [32–34], etc.

* Corresponding author.
E-mail address: hugeng@bit.edu.cn (G. Hu).

https://doi.org/10.1016/j.eml.2022.101789
2352-4316/

Acronyms

UM	Unimode
BM	Bimode
TM	Trimode
QM	Quadramode
PM	Pentamode
2D, 3D	Two- and three-dimensional
CFV	Characteristic force vector
EFC	Equifrequency contour
EFS	Equifrequency surface
FEA	Finite element analysis
PML	Perfectly matched layer
PBC	Periodic boundary condition
P-wave	Longitudinal wave
SV-wave	In-plane shear wave (motions are in the (x, y)-plane)
SH-wave	Anti-plane shear wave (motions are normal to the (x, y)-plane)

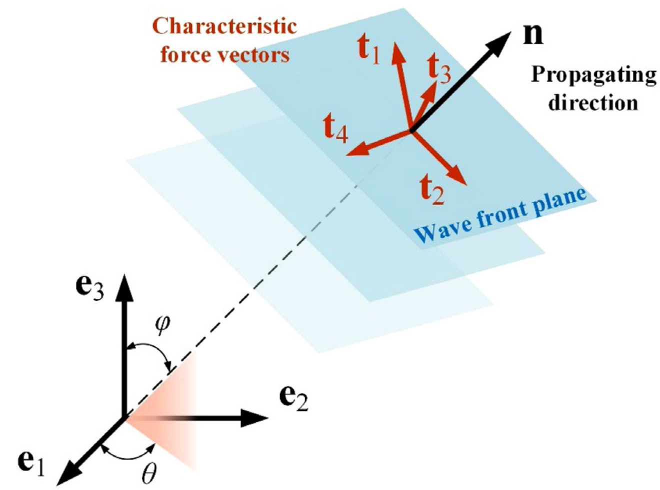

Fig. 1. Illustration of the CFVs of a BM material as an example and coordinate system in a 3D view.

The above exciting properties of extremal materials are benefiting from their unique slowness surfaces (or equifrequency surfaces, EFSs, which possess the same shape as the slowness surfaces) and from corresponding polarization characteristics. These extremal materials may offer an extraordinary capacity to shape their slowness surfaces, and in turn to monitor their wave characteristics. For example, there is only one slowness surface for the examined PM materials and two for the particular QM lattice. However, to what extent extremal materials can control the shape and the number of slowness surfaces has not been explored yet, the corresponding mechanisms are still unknown.

In this paper, we will examine in Section 2 the relationship between the number of hard modes (complementary to the soft modes) of the elastic matrix and the number of slowness surfaces one by one from PM to UM materials, and the condition whether the slowness surfaces are open along certain direction. In Section 3, several examples are given to illustrate our theoretical findings in Section 2. In Section 4, a broadband device of zero-refractive-index for elastic wave will be proposed with a TM material. In the end, conclusions are drawn in Section 5. The following acronyms will be used.

2. Theoretical analyses

2.1. Preliminary

According to Milton and Cherkaev [10], the fourth-order elasticity tensor of Cauchy elasticity with N zero energy modes is expressed in form of Kelvin's decomposition

$$\mathbf{C} = \sum_{i=1}^{6-N} K_i \mathbf{S}_i \otimes \mathbf{S}_i, \tag{1}$$

with K_i being the non-zero eigenvalues of the elasticity tensor, $\mathbf{S}_i$ being a second order symmetric tensor (characteristic stress relating to the hard mode). Eq. (1) indicates that such a material can support any stress in the subspace spanned by the $\mathbf{S}_i$. For convenience, the elasticity tensor can also be rewritten in a compact form as $\mathbf{C} = \sum_{i=1}^{6-N} \mathbf{S}_i \otimes \mathbf{S}_i$, where K_i is absorbed in $\mathbf{S}_i$. $\mathbf{S}_i$ will be written as a 2×2 or 3×3 symmetric matrix in the following for 2D or 3D cases, respectively.

In the following, we assume the moduli of the phases are independent of frequency. Then, for a 3D Cauchy elastic medium, in absence of body force, a time-harmonic elastic plane wave is governed by Christoffel's equation [35], which is given by

$$\boldsymbol{\Gamma} \cdot \mathbf{u} = \rho V^2 \mathbf{u}, \tag{2}$$

where $\boldsymbol{\Gamma} = \mathbf{n} \cdot \mathbf{C} \cdot \mathbf{n}$ is the acoustic tensor with $\mathbf{n}$ denoting the direction cosine of the wave vector $\mathbf{k}$, V denotes phase velocity ($V = \omega/|\mathbf{k}|$, ω is the angular frequency), $\mathbf{u}$ is displacement vector and ρ represents mass density of the elastic material. For a given unit vector of wave propagation direction $\mathbf{n}$, the phase velocity V is obtained by solving the eigenvalue λ ($\lambda = \rho V^2$) of the acoustic tensor matrix $\boldsymbol{\Gamma}$ from Eq. (2). With the help of Eq. (1), Christoffel's equation can be further rewritten as:

$$\left(\sum_{i=1}^{6-N} (\mathbf{n} \cdot \mathbf{S}_i) \otimes (\mathbf{S}_i \cdot \mathbf{n}) \right) \cdot \mathbf{u} = \rho V^2 \mathbf{u}. \tag{3}$$

Now, we define characteristic force vectors (CFVs for short) as:

$$\mathbf{t}_i = \mathbf{S}_i \cdot \mathbf{n}, \tag{4}$$

which represents the projection of the characteristic stress $\mathbf{S}_i$ on the wave front plane with normal $\mathbf{n}$, with $|\mathbf{n}| = 1$, as shown in Fig. 1. Then, the acoustic tensor can be rewritten as:

$$\boldsymbol{\Gamma} = \sum_{i=1}^{6-N} \mathbf{t}_i \otimes \mathbf{t}_i. \tag{5}$$

Generally, for a traditional Cauchy elastic medium with positive definite elasticity tensor, the number of non-zero eigenvalues λ of $\boldsymbol{\Gamma}$ in any direction $\mathbf{n}$ is always equal to the rank of $\boldsymbol{\Gamma}$, so there are always two closed slowness contours (or equifrequency contours, EFCs) for 2D and three closed slowness surfaces (or EFSs) for 3D, respectively [36,37]. If the eigenvalue λ is zero along some particular direction $\mathbf{n}$, which means zero phase speed V and infinite wave number, we call the slowness surface is opened along the direction $\mathbf{n}$. The number of openings along a given direction $\mathbf{n}$ is defined as the number of zero eigenvalues of $\boldsymbol{\Gamma}$ in this direction. It should be noticed that, if there is an opening at $\mathbf{n}$, there will also be an opening at $-\mathbf{n}$, but here the opposite direction is considered as a different direction. If the eigenvalue λ is not zero for any direction $\mathbf{n}$, the slowness surface is said to be closed. The characteristic equation of Eq. (2) is given for 3D cases by:

$$\lambda^3 - \operatorname{tr}(\boldsymbol{\Gamma})\,\lambda^2 + \operatorname{tr}\left(\boldsymbol{\Gamma}^A\right)\lambda - \det(\boldsymbol{\Gamma}) = 0, \tag{6}$$

where tr(·) and det(·) stand for the trace and determinant of a square matrix, the superscript A represents the adjugate matrix.

For traditional Cauchy elastic materials, there are six characteristic stresses orthogonal to each other, therefore there are at most six CFVs on the wave front plane. Here and in the following the orthogonality means the tensor inner product of any two characteristic stresses is zero [10] (e.g., $\mathbf{S}_1 : \mathbf{S}_2 = 0$). In Euclidean space, at most three of these six CFVs are linearly independent, we denote them by $\mathbf{t}_i$ ($i = 1, 2, 3$). According to the discussion will be given in the following, the coefficients in Eq. (6) can be summarized as

$$\begin{aligned}
&\mathrm{tr}\,(\boldsymbol{\Gamma}) = f_1\left(\left\{\mathbf{t}_i \cdot \mathbf{t}_j\right\}\right),\\
&\mathrm{tr}\left(\boldsymbol{\Gamma}^A\right) = f_2\left(\left\{\left(\mathbf{t}_i \times \mathbf{t}_j\right)^2\right\}\right),\\
&\det(\boldsymbol{\Gamma}) = f_3\left(\left[(\mathbf{t}_1 \times \mathbf{t}_2)\cdot \mathbf{t}_3\right]^2\right),\\
&(i, j = 1, 2, 3),
\end{aligned} \tag{7}$$

where f_1, f_2 and f_3 are appropriate linear functions of all combinations of their own arguments, i.e., the coefficients tr $(\boldsymbol{\Gamma})$, tr $(\boldsymbol{\Gamma}^A)$ and det $(\boldsymbol{\Gamma})$ are related to the scalar product, the vector product and the scalar triple product of the independent CFVs, respectively. Here and in the following the square of a vector represents its scalar product with itself (e.g., $\mathbf{t}^2 = \mathbf{t}\cdot\mathbf{t}$). Geometrically, these three coefficients are respectively related to the length of the independent CFV $\mathbf{t}_i$, the area of the parallelogram spanned by the $\left\{\mathbf{t}_i, \mathbf{t}_j\right\}$ and the volume of the parallelepiped spanned by the $\{\mathbf{t}_1, \mathbf{t}_2, \mathbf{t}_3\}$.

Eq. (7) shows clearly that the coefficients of the characteristic equation are sensitive to the geometric relationship of the independent CFVs. Extremal materials with rank-deficient elasticity tensor offer less characteristic stresses, this will affect the number and the geometric relationship of the independent CFVs on wave front plane, resulting in rich variation of the number and shape of slowness surfaces. This will be detailed in the following section.

2.2. Acoustic tensor for extremal materials

Firstly, we will consider PM materials, the simplest extremal materials of which five eigenvalues of their elasticity tensor are zero and support only stress proportional to their unique characteristic stress $\mathbf{S}_1$. There is only one CFV on any wave front plane with normal $\mathbf{n}$. According to Eqs. (2) and (4), the acoustic tensor $\boldsymbol{\Gamma}$ of PM materials can be expressed as

$$\boldsymbol{\Gamma} = \mathbf{t}_1 \otimes \mathbf{t}_1, \tag{8}$$

which implies that the $rank\,(\boldsymbol{\Gamma}) \le 1 = order\,(\boldsymbol{\Gamma}) - 2$. It is easy to derive that both tr$(\boldsymbol{\Gamma}^A)$ and det$(\boldsymbol{\Gamma})$ are always equal to zero [38] and $\mathrm{tr}\,(\boldsymbol{\Gamma}) = \mathbf{t}_1^2$ for arbitrary wave direction $\mathbf{n}$. As the unique characteristic stress $\mathbf{S}_1$ is not a null matrix, the CFV $\mathbf{t}_1$ cannot be always equal to zero for arbitrary $\mathbf{n}$ neither [39]. Therefore, according to Eq. (6), there is one and only one slowness surface for PM materials. And since $\lambda = \mathrm{tr}\,(\boldsymbol{\Gamma}) = \mathbf{t}_1^2$, the slowness surface opens along a given direction $\mathbf{n}^*$ if and only if $\mathbf{t}_1$ is equal to zero, i.e., $\mathbf{S}_1$ degenerates into a plane state in the plane $\mathbf{n}^*$, defined by $\mathbf{S}_1 \cdot \mathbf{n}^* = 0$. See Appendix A for proof.

Then, we will examine QM materials, which have four zero-eigenvalues of elasticity tensor and support any stress in the space spanned by two orthogonal characteristic stresses $\mathbf{S}_1$ and $\mathbf{S}_2$. The acoustic tensor $\boldsymbol{\Gamma}$ of QM materials can be expressed as:

$$\boldsymbol{\Gamma} = \mathbf{t}_1 \otimes \mathbf{t}_1 + \mathbf{t}_2 \otimes \mathbf{t}_2, \tag{9}$$

which implies that the $rank\,(\boldsymbol{\Gamma}) \le 2 = order\,(\boldsymbol{\Gamma}) - 1$. Thus det $(\boldsymbol{\Gamma})$ is always equal to zero for any $\mathbf{n}$ [38]. In this case, there are at most two non-zero eigenvalues in Eq. (6), so two slowness surfaces at most for QM materials, in agreement with the results predicted by another method [23].

We will analyze whether QM materials can always possess two slowness surfaces. If so, from Eq. (6), that means tr$(\boldsymbol{\Gamma}^A)$ cannot be always zero for any $\mathbf{n}$, i.e., the two CFVs $\mathbf{t}_1$ and $\mathbf{t}_2$ could not be always parallel to each other for any $\mathbf{n}$. This conclusion is straightforward since the two characteristic stresses are orthogonal, as detailed in Appendix B. Therefore, QM materials always possess two slowness surfaces (with the same results for 2D UM materials), and the coefficients of the characteristic equation can be collected as:

$$\begin{aligned}
&\mathrm{tr}\,(\boldsymbol{\Gamma}) = \mathbf{t}_1^2 + \mathbf{t}_2^2,\\
&\mathrm{tr}\left(\boldsymbol{\Gamma}^A\right) = (\mathbf{t}_1 \times \mathbf{t}_2)^2,\\
&\det(\boldsymbol{\Gamma}) = 0.
\end{aligned} \tag{10}$$

According to Eq. (10), for QM materials, the outer slowness surface is opened along a given $\mathbf{n}$ if and only if tr$(\boldsymbol{\Gamma}^A) = 0$, i.e., $\mathbf{t}_1$ is parallel to $\mathbf{t}_2$. And the two slowness surfaces are opened at the same time along a prescribed direction $\mathbf{n}$ if and only if tr$(\boldsymbol{\Gamma}) = 0$, i.e., $\mathbf{t}_1$ and $\mathbf{t}_2$ are both equal to $\mathbf{0}$. However, different from 3D QM materials, the inner slowness surface will never be opened for 2D UM materials (see Appendix C for proof).

Now, we will consider TM materials, which can bear any stress in the subspace spanned by three mutually orthogonal characteristic stress tensors $\mathbf{S}_1$, $\mathbf{S}_2$ and $\mathbf{S}_3$, respectively. They will have three corresponding CFVs $\mathbf{t}_1$, $\mathbf{t}_2$ and $\mathbf{t}_3$ on wave front plane.

If these three CFVs are always linearly independent, the acoustic tensor $\boldsymbol{\Gamma}$ of TM materials can be expressed as:

$$\boldsymbol{\Gamma} = \mathbf{t}_1 \otimes \mathbf{t}_1 + \mathbf{t}_2 \otimes \mathbf{t}_2 + \mathbf{t}_3 \otimes \mathbf{t}_3. \tag{11}$$

The coefficients of the characteristic equation for TM materials can then be simplified as:

$$\begin{aligned}
&\mathrm{tr}\,(\boldsymbol{\Gamma}) = \mathbf{t}_1^2 + \mathbf{t}_2^2 + \mathbf{t}_3^2,\\
&\mathrm{tr}\left(\boldsymbol{\Gamma}^A\right) = (\mathbf{t}_1 \times \mathbf{t}_2)^2 + (\mathbf{t}_2 \times \mathbf{t}_3)^2 + (\mathbf{t}_3 \times \mathbf{t}_1)^2,\\
&\det(\boldsymbol{\Gamma}) = \left[(\mathbf{t}_1 \times \mathbf{t}_2)\cdot \mathbf{t}_3\right]^2.
\end{aligned} \tag{12}$$

Then, in this case, there are three slowness surfaces. The opening of the slowness surfaces depend on geometric relationship between $\mathbf{t}_1$, $\mathbf{t}_2$ and $\mathbf{t}_3$. The outermost slowness surface is opened along a given $\mathbf{n}$ if and only if det$(\boldsymbol{\Gamma}) = 0$, i.e., $\mathbf{t}_1$, $\mathbf{t}_2$ and $\mathbf{t}_3$ are coplanar. And the middle together with the outermost slowness surfaces are opened at the same time along a prescribed $\mathbf{n}$ if and only if tr$(\boldsymbol{\Gamma}^A) = 0$, i.e., $\mathbf{t}_1$, $\mathbf{t}_2$ and $\mathbf{t}_3$ are parallel to each other. While, in this case, the innermost slowness surface is always closed, i.e., tr$(\boldsymbol{\Gamma})$ cannot be zero for any $\mathbf{n}$ (see Appendix D for proof).

Interestingly, if not so, it will degenerate into the case where these three CFVs are always linearly dependent, i.e., coplanar for any $\mathbf{n}$, as also demonstrated in Appendix D. In this case, there are only two slowness surfaces for such TM materials, with wave characteristics similar to QM materials.

Fourthly, the BM materials will be examined, which have two easy deformation modes and its acoustic tensor is expressed as:

$$\boldsymbol{\Gamma} = \mathbf{t}_1 \otimes \mathbf{t}_1 + \mathbf{t}_2 \otimes \mathbf{t}_2 + \mathbf{t}_3 \otimes \mathbf{t}_3 + \mathbf{t}_4 \otimes \mathbf{t}_4. \tag{13}$$

We will analyze whether BM materials always possess three slowness surfaces. From Eq. (6), that means det$(\boldsymbol{\Gamma})$ is not always zero, or the four CFVs $\{\mathbf{t}_1, \mathbf{t}_2, \mathbf{t}_3, \mathbf{t}_4\}$ cannot be always coplanar. As demonstrated in Appendix E, the $\{\mathbf{t}_1, \mathbf{t}_2, \mathbf{t}_3, \mathbf{t}_4\}$ cannot be always coplanar for any $\mathbf{n}$, indicating that BM materials always have three slowness surfaces.

In this case, we take $\{\mathbf{t}_1, \mathbf{t}_2, \mathbf{t}_3\}$ as the three independent CFVs and express $\mathbf{t}_4$ in term of them, we get for BM materials:

$$\mathrm{tr}\,(\boldsymbol{\Gamma}) = \mathbf{t}_1^2 + \mathbf{t}_2^2 + \mathbf{t}_3^2 + \left(\sum_{i=1}^{3} \alpha_i \mathbf{t}_i\right)^2,$$

$$\mathrm{tr}\left(\boldsymbol{\Gamma}^{A}\right)=\frac{1}{2}\sum_{\substack{i,j,k=1\\ i\neq j\neq k}}^{3}\left(\mathbf{t}_i\times\mathbf{t}_j\right)^2+\left(\alpha_i\left(\mathbf{t}_i\times\mathbf{t}_k\right)+\alpha_j\left(\mathbf{t}_j\times\mathbf{t}_k\right)\right)^2, \tag{14}$$
$$\det\left(\boldsymbol{\Gamma}\right)=\left(1+\sum_{i=1}^{3}\alpha_i^2\right)\left[\left(\mathbf{t}_1\times\mathbf{t}_2\right)\cdot\mathbf{t}_3\right]^2,$$

where

$$\mathbf{t}_4=\alpha_1\mathbf{t}_1+\alpha_2\mathbf{t}_2+\alpha_3\mathbf{t}_3\Leftrightarrow\begin{bmatrix}\alpha_1\\ \alpha_2\\ \alpha_3\end{bmatrix}=\begin{bmatrix}\mathbf{t}_1 & \mathbf{t}_2 & \mathbf{t}_3\end{bmatrix}^{-1}\mathbf{t}_4. \tag{15}$$

We also demonstrated in Appendix E that the four CFVs cannot be all zero along some $\mathbf{n}$, i.e., $\mathrm{tr}(\boldsymbol{\Gamma})\neq 0$, indicating from Eq. (6) that BM materials possess at least one non-zero eigenvalue and the innermost slowness surface is always closed.

As consequence, the outermost slowness surface of BM materials is opened if and only if $\det(\boldsymbol{\Gamma})$ is equal to zero. And both the middle and outermost slowness surfaces are opened together if and only if $\mathrm{tr}(\boldsymbol{\Gamma}^A)$ is equal to $\mathbf{0}$. While, as a result of fact that $\mathrm{tr}(\boldsymbol{\Gamma})$ is always non-zero, the innermost slowness surface will be never opened.

Finally, we will consider UM materials, which have five characteristic stresses and only one easy deformation mode, their acoustic tensor is given by:

$$\boldsymbol{\Gamma}=\mathbf{t}_1\otimes\mathbf{t}_1+\mathbf{t}_2\otimes\mathbf{t}_2+\mathbf{t}_3\otimes\mathbf{t}_3+\mathbf{t}_4\otimes\mathbf{t}_4+\mathbf{t}_5\otimes\mathbf{t}_5. \tag{16}$$

Through the previous analysis of BM materials, there are always three independent CFVs in UM materials, implying they always possess three slowness surfaces. As for BM materials, we express $\mathbf{t}_4$ and $\mathbf{t}_5$ with the three independent CFVs, the coefficients of the characteristic equation of UM materials can be collected as:

$$\begin{aligned}\mathrm{tr}\left(\boldsymbol{\Gamma}\right)&=\mathbf{t}_1^2+\mathbf{t}_2^2+\mathbf{t}_3^2+\left(\sum_{i=1}^{3}\alpha_i\mathbf{t}_i\right)^2+\left(\sum_{i=1}^{3}\beta_i\mathbf{t}_i\right)^2,\\ \mathrm{tr}\left(\boldsymbol{\Gamma}^{A}\right)&=\left(\begin{aligned}&\frac{1}{2}\sum_{i,j=1}^{3}\left[\left(1+\eta_i^2\right)\left(1+\eta_j^2\right)-\left(\eta_i\eta_j\right)^2\right]\left(\mathbf{t}_i\times\mathbf{t}_j\right)^2\\ &+\sum_{\substack{i,j,k=1\\ i\neq j\neq k}}^{3}\left[\left(1+\eta_i^2\right)\left(\eta_j\eta_k\right)-\left(\eta_i\eta_j\right)\left(\eta_i\eta_k\right)\right]\\ &\times\left(\mathbf{t}_i\times\mathbf{t}_j\right)\cdot\left(\mathbf{t}_i\times\mathbf{t}_k\right)\end{aligned}\right),\\ \det\left(\boldsymbol{\Gamma}\right)&=\left(\begin{aligned}&\prod_{i=1}^{3}\left(1+\eta_i^2\right)-\frac{1}{2}\sum_{\substack{i,j,k=1\\ i\neq j\neq k}}^{3}\left(1+\eta_i^2\right)\left(\eta_j\eta_k\right)^2\\ &+2\left(\eta_1\eta_2\right)\left(\eta_1\eta_3\right)\left(\eta_2\eta_3\right)\end{aligned}\right)\\ &\quad\times\left[\left(\mathbf{t}_1\times\mathbf{t}_2\right)\cdot\mathbf{t}_3\right]^2,\end{aligned} \tag{17}$$

where α is the same as Eq. (15), β and $(\eta_i\eta_j)$ is defined by

$$\begin{aligned}&\mathbf{t}_5=\beta_1\mathbf{t}_1+\beta_2\mathbf{t}_2+\beta_3\mathbf{t}_3\Leftrightarrow\begin{bmatrix}\beta_1\\ \beta_2\\ \beta_3\end{bmatrix}=\begin{bmatrix}\mathbf{t}_1 & \mathbf{t}_2 & \mathbf{t}_3\end{bmatrix}^{-1}\mathbf{t}_5,\\ &\left(\eta_i\eta_j\right)=\alpha_i\alpha_j+\beta_i\beta_j.\end{aligned} \tag{18}$$

For UM materials, the outermost slowness surface is opened if and only if the $\det(\boldsymbol{\Gamma})$ is equal to zero.

In the following sections, we will provide some concrete examples to illustrate the theoretical results, and some specific wave function will also be explained with TM elastic metamaterials.

3. Illustrating examples

In this section, several examples from PM to UM materials will be presented in sequence in order to illustrate our previous theoretical findings. For convenience, the hard modes of different classes of extremal materials are carefully selected so that the following four propagation directions can give more possibilities for the opening and closing of slowness surfaces:

$$\begin{aligned}\mathbf{n}_1&=\begin{bmatrix}1 & 0 & 0\end{bmatrix}^T,\\ \mathbf{n}_2&=\begin{bmatrix}0 & 1 & 0\end{bmatrix}^T,\\ \mathbf{n}_3&=\begin{bmatrix}0 & 0 & 1\end{bmatrix}^T,\\ \mathbf{n}_4&=\frac{\sqrt{2}}{2}\begin{bmatrix}1 & 1 & 0\end{bmatrix}^T.\end{aligned} \tag{19}$$

Firstly, we consider a PM material with the following characteristic stress:

$$\mathbf{S}_1=\begin{bmatrix}0 & 0 & 0\\ 0 & 1 & 0\\ 0 & 0 & 1\end{bmatrix}, \tag{20}$$

which indicates that such PM material can only support a hydrostatic pressure in the (y,z)-plane. Here, without loss of generality, we set the components S_{yy} and S_{zz} in Eq. (20) to unit. Its slowness surface is shown in Fig. 2(a), there is only one slowness surface. Besides, since the CFV $\mathbf{t}_1$ is zero along $\mathbf{n}_1$, $\mathrm{tr}(\boldsymbol{\Gamma})$ is zero too in this case, so the slowness surface is opened along $\mathbf{n}_1$. While it is closed along any other propagation direction (not parallel to $\mathbf{n}_1$, such as $\mathbf{n}_3$), because in these directions $\mathbf{t}_1$ and $\mathrm{tr}(\boldsymbol{\Gamma})$ are no longer equal to zero. The details of $\mathrm{tr}(\boldsymbol{\Gamma})$, $\mathrm{tr}(\boldsymbol{\Gamma}^A)$, $\det(\boldsymbol{\Gamma})$ and $\mathbf{t}_1$ are summarized in Table 1 for such PM material, as well as QM, TM, BM and UM materials for completeness.

Then, we will consider a QM material which is stiff to any stress in the subspace spanned by the following two orthogonal characteristic stress tensors $\mathbf{S}_1$ and $\mathbf{S}_2$:

$$\mathbf{S}_1=\begin{bmatrix}2 & 0 & 0\\ 0 & 2 & 0\\ 0 & 0 & 0\end{bmatrix},\mathbf{S}_2=\begin{bmatrix}0 & 1 & 0\\ 1 & 0 & 0\\ 0 & 0 & 0\end{bmatrix}. \tag{21}$$

The slowness surfaces of such QM material is shown in Fig. 2(b), indicating that there are only two slowness surfaces there. Since $\mathbf{t}_1$ and $\mathbf{t}_2$ are neither parallel to each other nor equal to zero in the direction $\mathbf{n}_1$, both $\mathrm{tr}(\boldsymbol{\Gamma})$ and $\mathrm{tr}(\boldsymbol{\Gamma}^A)$ in Eq. (10) are non-zero, the innermost and middle slowness surfaces are closed along $\mathbf{n}_1$. While the outer slowness surface is opened along $\mathbf{n}_4$, because $\mathbf{t}_1$ and $\mathbf{t}_2$ are parallel but both non-zero, driving $\mathrm{tr}(\boldsymbol{\Gamma}^A)$ to zero in this direction. Besides, in the direction $\mathbf{n}_3$, due to the fact that $\mathbf{t}_1$ and $\mathbf{t}_2$ are both equal to zero, leading to three zero-eigenvalues for Eq. (10), the remaining two slowness surfaces are opened at the same time. The details of numerical results of the coefficients in Eq. (6) are summarized in Table 1.

Thirdly, a TM material with the following characteristic stresses is considered:

$$\mathbf{S}_1=\begin{bmatrix}1 & 0 & 0\\ 0 & 0 & 0\\ 0 & 0 & 0\end{bmatrix},\mathbf{S}_2=\begin{bmatrix}0 & 0 & 0\\ 0 & 0 & 1\\ 0 & 1 & 0\end{bmatrix},\mathbf{S}_3=\begin{bmatrix}0 & 1 & 0\\ 1 & 0 & 0\\ 0 & 0 & 0\end{bmatrix}. \tag{22}$$

According to the analysis in Section 2, such TM material will possess three slowness surfaces, as shown in Fig. 2(c). Since the CFVs $\{\mathbf{t}_1,\mathbf{t}_2,\mathbf{t}_3\}$ are coplanar in the plane $\mathbf{n}_1$, $\det(\boldsymbol{\Gamma})$ in Eq. (12) is zero in this case, then the outermost slowness surface is opened. While, in the direction $\mathbf{n}_3$, the middle and the outermost slowness surfaces are opened at the same time. Because the CFVs $\{\mathbf{t}_1,\mathbf{t}_2,\mathbf{t}_3\}$ are parallel to each other, driving both $\det(\boldsymbol{\Gamma})$ and $\mathrm{tr}(\boldsymbol{\Gamma}^A)$ to zero. Moreover, because of linear independence of the CFVs $\{\mathbf{t}_1,\mathbf{t}_2,\mathbf{t}_3\}$ in the direction $\mathbf{n}_4$, all the three slowness surfaces are closed.

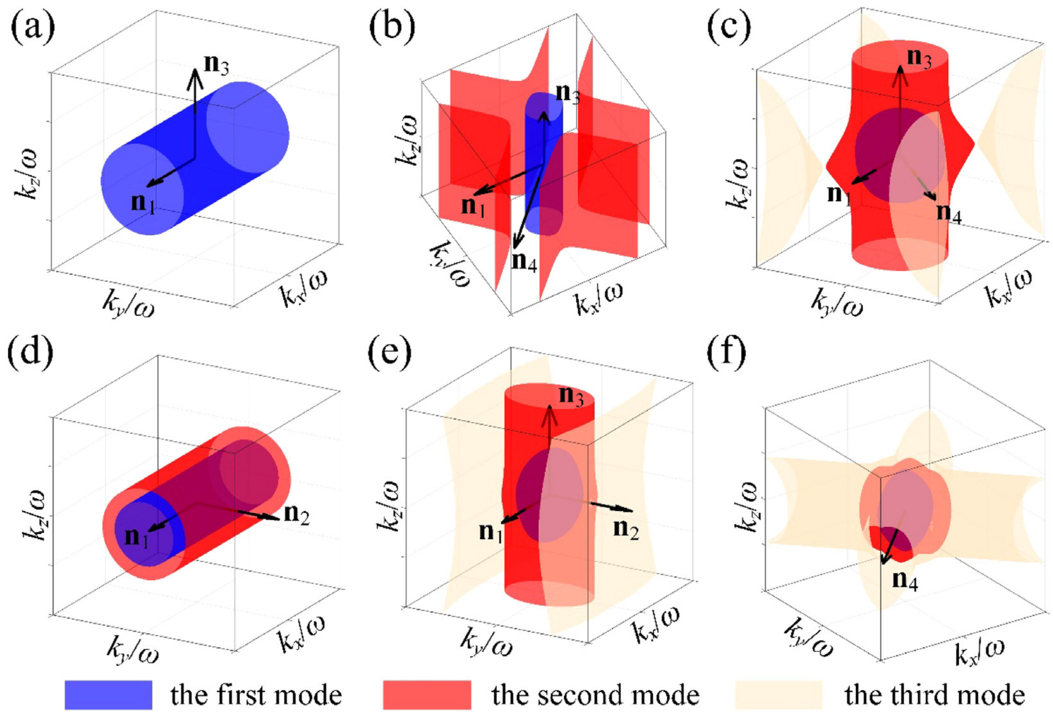

Fig. 2. Slowness surfaces for different classes of extremal materials: (a) PM with Eq. (20); (b) QM with Eq. (21); (c) TM with Eq. (22); (d) TM with Eq. (23); (e) BM with Eq. (24); (f) UM with Eq. (25).

Table 1
The coefficients in Eq. (6) for different extremal material examples.

Type (Num. EFSs)	Directions	CFVs and coefficients	Num. zero-eigenvalues	Num. openings
PM (1)	$\mathbf{n}_1$	$\mathbf{t}=\mathbf{0}$; $\mathrm{tr}(\boldsymbol{\Gamma})=0$; $\mathrm{tr}(\boldsymbol{\Gamma}^A)=0$; $\det(\boldsymbol{\Gamma})=0$	3	1
	$\mathbf{n}_3$	$\mathbf{t}=[0,0,1]^{\mathrm{T}}$; $\mathrm{tr}(\boldsymbol{\Gamma})=1$; $\mathrm{tr}(\boldsymbol{\Gamma}^A)=0$; $\det(\boldsymbol{\Gamma})=0$	2	0
QM (2)	$\mathbf{n}_1$	$\mathbf{t}_1=[2,0,0]^{\mathrm{T}}$; $\mathbf{t}_2=[0,1,0]^{\mathrm{T}}$; $\mathrm{tr}(\boldsymbol{\Gamma})=5$; $\mathrm{tr}(\boldsymbol{\Gamma}^A)=4$; $\det(\boldsymbol{\Gamma})=0$	1	0
	$\mathbf{n}_3$	$\mathbf{t}_1=\mathbf{t}_2=\mathbf{0}$; $\mathrm{tr}(\boldsymbol{\Gamma})=0$; $\mathrm{tr}(\boldsymbol{\Gamma}^A)=0$; $\det(\boldsymbol{\Gamma})=0$	3	2
	$\mathbf{n}_4$	$\mathbf{t}_1=2\mathbf{t}_2=[\sqrt{2},\ \sqrt{2},\ 0]^{\mathrm{T}}$; $\mathrm{tr}(\boldsymbol{\Gamma})=5$; $\mathrm{tr}(\boldsymbol{\Gamma}^A)=0$; $\det(\boldsymbol{\Gamma})=0$	2	1
TM1 (3)	$\mathbf{n}_1$	$\mathbf{t}_1=[1,0,0]^{\mathrm{T}}$; $\mathbf{t}_2=\mathbf{0}$; $\mathbf{t}_3=[0,1,0]^{\mathrm{T}}$; $\mathrm{tr}(\boldsymbol{\Gamma})=2$; $\mathrm{tr}(\boldsymbol{\Gamma}^A)=1$; $\det(\boldsymbol{\Gamma})=0$	1	1
	$\mathbf{n}_3$	$\mathbf{t}_1=\mathbf{0}$; $\mathbf{t}_2=[0,1,0]^{\mathrm{T}}$; $\mathbf{t}_3=\mathbf{0}$; $\mathrm{tr}(\boldsymbol{\Gamma})=1$; $\mathrm{tr}(\boldsymbol{\Gamma}^A)=0$; $\det(\boldsymbol{\Gamma})=0$	2	2
	$\mathbf{n}_4$	$\mathbf{t}_1=[\sqrt{2}/2,0,0]^{\mathrm{T}}$; $\mathbf{t}_2=[0,0,\ \sqrt{2}/2]^{\mathrm{T}}$; $\mathbf{t}_3=[\sqrt{2}/2,\ \sqrt{2}/2,0]^{\mathrm{T}}$; $\mathrm{tr}(\boldsymbol{\Gamma})=2$; $\mathrm{tr}(\boldsymbol{\Gamma}^A)=1$; $\det(\boldsymbol{\Gamma})=1/8$	0	0
TM2 (2)	$\mathbf{n}_1$	$\mathbf{t}_1=\mathbf{t}_2=\mathbf{t}_3=\mathbf{0}$; $\mathrm{tr}(\boldsymbol{\Gamma})=0$; $\mathrm{tr}(\boldsymbol{\Gamma}^A)=0$; $\det(\boldsymbol{\Gamma})=0$	3	2
	$\mathbf{n}_2$	$\mathbf{t}_1=\mathbf{t}_2=[0,1,0]^{\mathrm{T}}$; $\mathbf{t}_3=[0,0,1]^{\mathrm{T}}$; $\mathrm{tr}(\boldsymbol{\Gamma})=3$; $\mathrm{tr}(\boldsymbol{\Gamma}^A)=2$; $\det(\boldsymbol{\Gamma})=0$	1	0
BM (3)	$\mathbf{n}_1$	$\mathbf{t}_1=[\sqrt{2},0,0]^{\mathrm{T}}$; $\mathbf{t}_2=\mathbf{t}_3=\mathbf{0}$; $\mathbf{t}_4=[0,1,0]^{\mathrm{T}}$; $\mathrm{tr}(\boldsymbol{\Gamma})=3$; $\mathrm{tr}(\boldsymbol{\Gamma}^A)=2$; $\det(\boldsymbol{\Gamma})=0$	1	1
	$\mathbf{n}_2$	$\mathbf{t}_1=\mathbf{0}$; $\mathbf{t}_2=[0,\ \sqrt{2},0]^{\mathrm{T}}$; $\mathbf{t}_3=[0,0,1]^{\mathrm{T}}$; $\mathbf{t}_4=[1,0,0]^{\mathrm{T}}$; $\mathrm{tr}(\boldsymbol{\Gamma})=4$; $\mathrm{tr}(\boldsymbol{\Gamma}^A)=5$; $\det(\boldsymbol{\Gamma})=2$	0	0
	$\mathbf{n}_3$	$\mathbf{t}_1=\mathbf{t}_2=\mathbf{t}_4=\mathbf{0}$; $\mathbf{t}_3=[0,1,0]^{\mathrm{T}}$; $\mathrm{tr}(\boldsymbol{\Gamma})=1$; $\mathrm{tr}(\boldsymbol{\Gamma}^A)=0$; $\det(\boldsymbol{\Gamma})=0$	2	2
UM (3)	$\mathbf{n}_4$	$\mathbf{t}_1=\sqrt{2}\mathbf{t}_5=[1,1,0]^{\mathrm{T}}$; $\mathbf{t}_3=\mathbf{t}_4=[0,0,\ \sqrt{2}/2]^{\mathrm{T}}$; $\mathbf{t}_2=\mathbf{0}$; $\mathrm{tr}(\boldsymbol{\Gamma})=4$; $\mathrm{tr}(\boldsymbol{\Gamma}^A)=3$; $\det(\boldsymbol{\Gamma})=0$	1	1

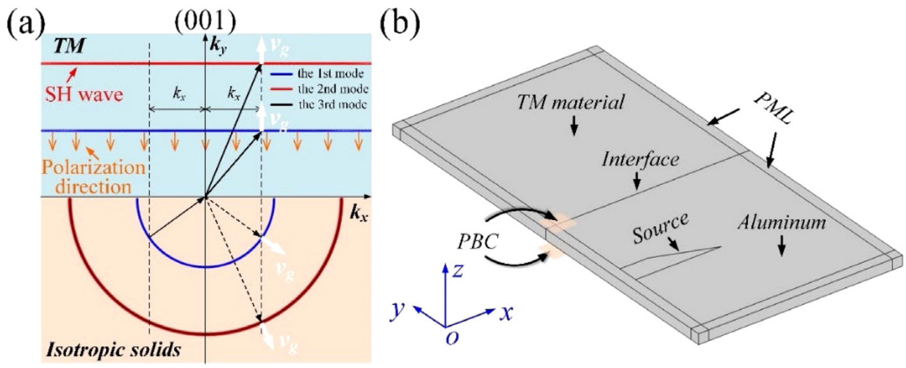

Fig. 3. EFC analysis and FEA method: (a) EFCs in the (001) plane of isotropic solid (bottom) and TM material (top); (b) FE model used in COMSOL. . (For interpretation of the references to color in this figure legend, the reader is referred to the web version of this article.)

The next one we will consider is a TM material, which is stiff to any stress in the (y, z)-plane:

$$\mathbf{S}_1=\begin{bmatrix}0&0&0\\0&1&0\\0&0&1\end{bmatrix},\mathbf{S}_2=\begin{bmatrix}0&0&0\\0&1&0\\0&0&-1\end{bmatrix},\mathbf{S}_3=\begin{bmatrix}0&0&0\\0&0&1\\0&1&0\end{bmatrix}. \quad (23)$$

According to the analysis in Section 2, such TM material will possess only two slowness surfaces instead of three, as shown in Fig. 2(d). Since the CFVs $\{\mathbf{t}_1, \mathbf{t}_2, \mathbf{t}_3\}$ are zero along $\mathbf{n}_1$, $\mathrm{tr}(\mathbf{\Gamma})$ in Eq. (12) is zero and the slowness surfaces are both opened. While, it is closed along any other propagation direction (not parallel to $\mathbf{n}_1$, such as $\mathbf{n}_2$). Because there are always two linearly independent CFVs in $\{\mathbf{t}_1, \mathbf{t}_2, \mathbf{t}_3\}$ along these directions, so that $\mathrm{tr}(\mathbf{\Gamma})$ and $\mathrm{tr}(\mathbf{\Gamma}^A)$ are no longer equal to zero. The details of numerical results of the coefficients in Eqs. (22) and (23) are summarized in Table 1 as TM1 and TM2, respectively.

Now, let us consider a BM material, which has two easy deformation modes and its characteristic stresses are designed as:

$$\mathbf{S}_1=\begin{bmatrix}\sqrt{2}&0&0\\0&0&0\\0&0&0\end{bmatrix},\mathbf{S}_2=\begin{bmatrix}0&0&0\\0&\sqrt{2}&0\\0&0&0\end{bmatrix},\mathbf{S}_3=\begin{bmatrix}0&0&0\\0&0&1\\0&1&0\end{bmatrix},$$
$$\mathbf{S}_4=\begin{bmatrix}0&1&0\\1&0&0\\0&0&0\end{bmatrix}. \quad (24)$$

Fig. 2(e) shows the slowness surfaces of such BM material, indicating there are three slowness surfaces there. Since $\{\mathbf{t}_1, \mathbf{t}_2, \mathbf{t}_3, \mathbf{t}_4\}$ are parallel to each other in the direction $\mathbf{n}_3$, both $\mathrm{tr}(\mathbf{\Gamma}^A)$ and $\det(\mathbf{\Gamma})$ in Eq. (14) are zero, then the middle and the outermost slowness surfaces are opened. However, only the outermost slowness surface is opened along $\mathbf{n}_1$, because the CFVs $\{\mathbf{t}_1, \mathbf{t}_2, \mathbf{t}_3, \mathbf{t}_4\}$ are coplanar along $\mathbf{n}_1$, leading $\det(\mathbf{\Gamma})$ to zero. Apart from this, in the direction $\mathbf{n}_2$, due to the fact that there are three linearly independent CFVs in $\{\mathbf{t}_1, \mathbf{t}_2, \mathbf{t}_3, \mathbf{t}_4\}$, all the slowness surfaces are closed.

Finally, a UM material with the following characteristic stresses is considered:

$$\mathbf{S}_1=\begin{bmatrix}\sqrt{2}&0&0\\0&\sqrt{2}&0\\0&0&0\end{bmatrix},\mathbf{S}_2=\begin{bmatrix}0&0&0\\0&0&0\\0&0&1\end{bmatrix},\mathbf{S}_3=\begin{bmatrix}0&0&0\\0&0&1\\0&1&0\end{bmatrix},$$
$$\mathbf{S}_4=\begin{bmatrix}0&0&1\\0&0&0\\1&0&0\end{bmatrix},\mathbf{S}_5=\begin{bmatrix}0&1&0\\1&0&0\\0&0&0\end{bmatrix}. \quad (25)$$

The slowness surfaces for such UM material are shown in Fig. 2(f). When wave propagates in the direction $\mathbf{n}_4$, the CFVs $\{\mathbf{t}_1, \mathbf{t}_2, \mathbf{t}_3, \mathbf{t}_4, \mathbf{t}_5\}$ are coplanar, so $\det(\mathbf{\Gamma})$ is zero. As a result, the outermost slowness surface is opened in this direction, as expected.

4. Zero-refractive-index device for elastic waves

In the following, we will take TM materials as an example, and explore their potential in designing broadband zero-refractive-index device for elastic waves, useful for energy collection. In particular, for the convenience of subsequent numerical validation, the characteristic stresses $\mathbf{S}_1$, $\mathbf{S}_2$, and $\mathbf{S}_3$ are multiplied respectively by $\sqrt{5.26}\times 10^5$, $\sqrt{5.26}\times 10^5$ and $\sqrt{2.67}\times 10^5$, and the density is $\rho^{TM} = 2700$ kg/m^3. Thus, the elastic matrix of this TM material in Voigt notation reads:

$$C^{TM}=\begin{bmatrix}0&0&0&0&0&0\\0&105.2&0&0&0&0\\0&0&105.2&0&0&0\\0&0&0&26.7&0&0\\0&0&0&0&0&0\\0&0&0&0&0&0\end{bmatrix}\ \mathrm{GPa}. \quad (26)$$

Fig. 3(a) shows the slowness curves of the calculated refraction and reflection at an interface in the (001) plane (i.e., the (k_x, k_y)-plane with $k_z = 0$) between the semi-infinite homogeneous TM material (top) with the hard modes given by Eq. (23), as well as an isotropic solid (bottom) with the material constants as follows: $C_{11}^{ISO} = 105.2$ GPa, $C_{12}^{ISO} = 51.8$ GPa, the density $\rho^{ISO} = \rho^{TM}$ (aluminum). The orange arrows in Fig. 3(a) represent the polarization of the first mode of the TM material. We can see that no matter what type of elastic wave is incident at whatever angle, the group velocity (white arrows in Fig. 3(a)) of the transmitted wave is always parallel to k_y-axis, implying zero-refractive-index for the elastic waves. It should be noticed that, since in this case one in-plane mode vanishing in the (001) plane of the TM material, there would be a discontinuity in the displacement at the interface. Benefiting from the decoupling between the in-plane and out-of-plane modes, at the interface between the isotropic material and TM material, the continuity conditions for the in-plane modes can be established by following the method proposed by Zheng et al. [29].

Numerical simulation was conducted by commercial finite element analysis (FEA) software COMSOL Multiphysics 5.6. In the simulation, as shown in Fig. 3(b), the surroundings of the computed domain are covered by perfectly matched layers (PMLs) to eliminate wave reflection. The total size of the model in Fig. 3(b) is 300 mm × 600 mm × 15 mm. Since the homogeneous TM material is also a kind of linear Cauchy elastic materials, the PMLs of Solid Mechanics Module in COMSOL can still work. Periodic boundary conditions (PBCs) are imposed on the top and bottom surfaces of the model.

In order to illustrate the property of zero-refractive-index with the TM material, we perform calculations on wave propagation for an obliquely incident Gaussian beam initiated from

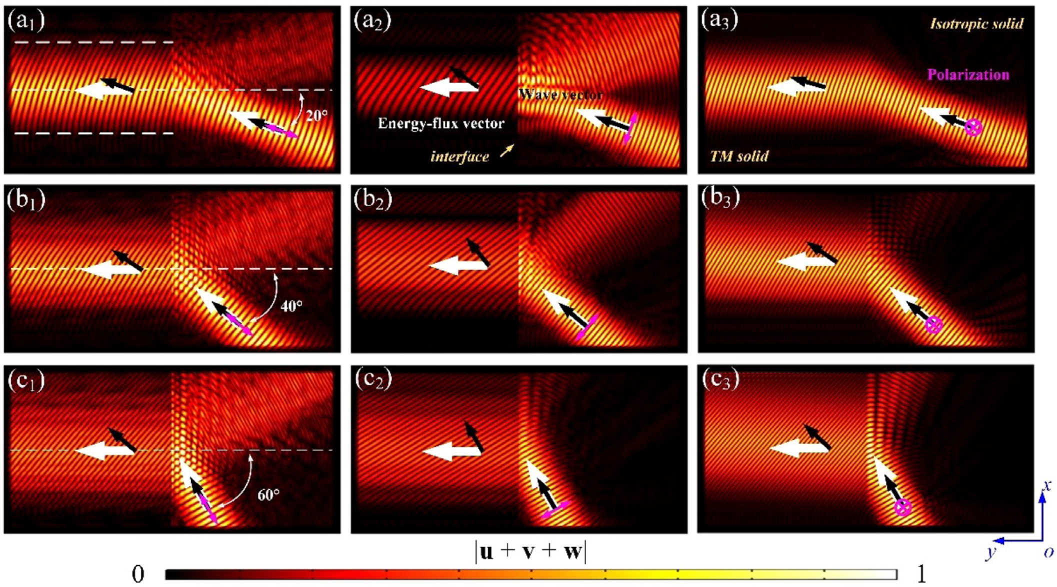

Fig. 4. Wave propagation for obliquely incident waves initiated from isotropic solid to homogeneous TM material: (a_1), (a_2) and (a_3) for P-, SV- and SH-waves, respectively (the fields are normalized by the incident wave); both (b) and (c) are the same as (a) but with different incident angles.

the isotropic solid to the TM material, different wave types and incident angles are considered, including P-, SV- and SH-waves as well as incident angles 20°, 40° and 60°, respectively. The wave propagations represented by the normalized displacement fields are shown in Fig. 4. A line source to excite different types of elastic waves (P-, SV- and SH-wave) is located in the isotropic medium. The P- and SV/SH-Gaussian beams with frequency 300 kHz and 200 kHz are generated respectively. Fig. 4 shows clearly that, whatever the angles and wave types, Poynting (Energy-flux) vectors of the transmitted waves are always parallel to the normal of the interface, although the transmitted waves have different wave vectors. This locking phenomenon for transmitting energy orientation may be useful to energy harvesting in structures. The asymmetry in the reflected wave to the normal of the interface is due to particular mode conversion for the different incident waves. The above mechanism can function with a broad frequency band, since only static material properties are utilized without resonance.

5. Summary

The exotic properties of extremal elastic materials come from their extraordinary capacity in shaping slowness surfaces, including the reduction in number and opening of the slowness surfaces. We have examined these mechanisms by carefully inspecting the CFVs on the wave front plane. It is demonstrated that the number of the linearly independent CFVs determines the number of slowness surfaces, and the opening of these surfaces is governed by the vanishing of these vectors along particular directions. These theoretical findings are also illustrated by concrete examples for different classes of extremal elastic materials. Finally, a broadband device of zero-refractive-index for elastic wave is also proposed with a TM material. This work provides the first systematic study on the control ability on slowness surfaces by extremal materials, and offers a new prospective to design extremal metamaterials and to control low frequency elastic waves.

Declaration of competing interest

The authors declare that they have no known competing financial interests or personal relationships that could have appeared to influence the work reported in this paper.

Acknowledgments

We would like to thank professors Xiaoning Liu and Pingzhang Zhou for the discussions during this work, and the two reviewers for their constructive suggestions. The support of National Natural Science Foundation of China (Grants No. 11632003, No. 11972083, No. 11991030) is also acknowledged.

Appendix A

Proposition: for any symmetric non-zero second order tensor $\mathbf{S}$, the necessary and sufficient condition for any vector defined by $\mathbf{t} = \mathbf{S}{\cdot}\mathbf{n}$ to be always lying in certain plane with normal $\mathbf{m}$ is that $\mathbf{S}$ degenerates into a plane state defined by $\mathbf{S}\cdot\mathbf{m} = \mathbf{0}$.

Demonstration: if a tensor $\mathbf{S}$ is of a plane state with a plane $\mathbf{m}$, we would have:

$$\mathbf{S}\cdot\mathbf{m} = \mathbf{0}. \tag{A.1}$$

Benefiting from the symmetry of the tensor $\mathbf{S}$, the scalar product of $\mathbf{t}$ and $\mathbf{m}$ gives:

$$\mathbf{t}\cdot\mathbf{m} = (\mathbf{S}\cdot\mathbf{n})\cdot\mathbf{m} \overset{\mathbf{S}=\mathbf{S}^T}{=} (\mathbf{S}\cdot\mathbf{m})\cdot\mathbf{n} = \mathbf{0}\cdot\mathbf{n} = 0,\ \forall\mathbf{n}. \tag{A.2}$$

We have thus proved that any vector $\mathbf{t}$ always lies in such plane $\mathbf{m}$.

Conversely if the vector $\mathbf{t}$ always lies in a plane $\mathbf{m}$, we would have:

$$\mathbf{t}\cdot\mathbf{m} = (\mathbf{S}\cdot\mathbf{n})\cdot\mathbf{m} \overset{\mathbf{S}=\mathbf{S}^T}{=} (\mathbf{S}\cdot\mathbf{m})\cdot\mathbf{n} = 0,\ \forall\mathbf{n}. \tag{A.3}$$

Since Eq. (A.3) holds for any $\mathbf{n}$, the coefficient matrix should be a zero matrix, leading to:

$$\mathbf{S}\cdot\mathbf{m} = \mathbf{0}. \tag{A.4}$$

Therefore, the proposition holds. The proposition is also true for 2D cases. In this case $\mathbf{S}$ degenerates into a uniaxial state.

Appendix B

Proposition: two symmetric non-zero second order tensors $\mathbf{S}_1$ and $\mathbf{S}_2$ mutually orthogonal to each other, any two vectors defined by

$\mathbf{t}_i = \mathbf{S}_i \cdot \mathbf{n}$ (i = 1, 2), cannot be always parallel to each other for any $\mathbf{n}$.

Demonstration: if the vectors $\mathbf{t}_1$ and $\mathbf{t}_2$ are always parallel, we would have

$$\mathbf{t}_1 \times \mathbf{t}_2 \equiv 0 \Leftrightarrow (\mathbf{S}_1 \cdot \mathbf{n}) \times (\mathbf{S}_2 \cdot \mathbf{n}) \equiv 0, \forall \mathbf{n}. \tag{B.1}$$

Any symmetric tensor $\mathbf{S}$ has at least one principal frame, i.e., a right-handed triplet of orthogonal principal directions [39]. In order to facilitate the analysis, a Cartesian coordinate system $\{\mathbf{e}_i\}$ is chosen to coincide with the principal axes of $\mathbf{S}_1$. Then, $\mathbf{S}_1$ has only diagonal elements (i.e., the off-diagonal elements of $\mathbf{S}_1$ are all zero) [39], while $\mathbf{S}_2$ is expressed in a general form:

$$\begin{aligned} &\mathbf{S}_1 = S_{11}^{(1)}\mathbf{e}_1\mathbf{e}_1 + S_{22}^{(1)}\mathbf{e}_2\mathbf{e}_2 + S_{33}^{(1)}\mathbf{e}_3\mathbf{e}_3, \\ &\mathbf{S}_2 = \sum_{i,j=1}^{3} S_{ij}^{(2)}\mathbf{e}_i\mathbf{e}_j. \end{aligned} \tag{B.2}$$

Substituting Eq. (B.2) into Eq. (B.1), and noting that the relation holds for arbitrary $\mathbf{n}$, the collected coefficients of the components $n_i n_j$ should all be zero. With the help of Eq. (B.2) and the orthogonality between the tensors $\mathbf{S}_1$ and $\mathbf{S}_2$ (i.e., $\mathbf{S}_1$: $\mathbf{S}_2$ = 0, the last constraint condition in Eq. (B.3)), we can get the following constraint conditions for the two tensors as:

$$\begin{bmatrix} & S_{12}^{(2)}\mathbf{I}_{3\times 3} & \\ & S_{13}^{(2)}\mathbf{I}_{3\times 3} & \\ & S_{23}^{(2)}\mathbf{I}_{3\times 3} & \\ -S_{33}^{(2)} & 0 & S_{11}^{(2)} \\ S_{22}^{(2)} & -S_{11}^{(2)} & 0 \\ 0 & S_{33}^{(2)} & -S_{22}^{(2)} \\ S_{11}^{(2)} & S_{22}^{(2)} & S_{33}^{(2)} \end{bmatrix} \begin{bmatrix} S_{11}^{(1)} \\ S_{22}^{(1)} \\ S_{33}^{(1)} \end{bmatrix} = \mathbf{0}. \tag{B.3}$$

According to the definition of the rank of a matrix, since $\mathbf{S}_2$ is non-zero, the coefficient matrix in Eq. (B.3) has 3 linearly independent columns and hence has full column rank. Thus, $\mathbf{S}_1$ should be zero, which is contradictory to the definition. So, the proposition holds.

Appendix C

Proposition: For two 2D symmetric non-zero second order tensors $\mathbf{S}_1$ and $\mathbf{S}_2$ mutually orthogonal to each other, any two 2D vectors defined by $\mathbf{t}_i = \mathbf{S}_i \cdot \mathbf{n}$ (i = 1, 2) cannot be zero simultaneously.

Demonstration: if both $\mathbf{t}_1$ and $\mathbf{t}_2$ are equal to $\mathbf{0}$ with some $\mathbf{n}^*$, then we would have:

$$\mathbf{S}_1 \cdot \mathbf{n}^* = \mathbf{S}_2 \cdot \mathbf{n}^* = \mathbf{0}. \tag{C.1}$$

According to Appendix A, Eq. (C.1) implies both tensors $\mathbf{S}_1$ and $\mathbf{S}_2$ are of uniaxial states with the plane $\mathbf{n}^*$, then

$$rank\left(\left[S^{(1)}, S^{(2)}\right]\right) = 1, \tag{C.2}$$

where the second order tensor $\mathbf{S}$ is written into Voigt notation $\{S\} = \left\{S_{11} \quad S_{22} \quad \sqrt{2}S_{12}\right\}^T$. Therefore, the $\mathbf{S}_1$ and $\mathbf{S}_2$ are linearly dependent rather than mutually orthogonal each other, so the proposition holds.

The acoustic tensor of 2D UM materials reads as:

$$\lambda^2 - \mathrm{tr}\,(\boldsymbol{\Gamma})\,\lambda + \det(\boldsymbol{\Gamma}) = 0, \tag{C.3}$$

with

$$\begin{aligned} &\mathrm{tr}\,(\boldsymbol{\Gamma}) = \mathbf{t}_1^2 + \mathbf{t}_2^2, \\ &\det(\boldsymbol{\Gamma}) = (\mathbf{t}_1 \times \mathbf{t}_2)^2\,. \end{aligned} \tag{C.4}$$

As demonstrated previously, $\mathrm{tr}\,(\boldsymbol{\Gamma}) \neq 0$ for any $\mathbf{n}$, so the inner slowness curve will never be opened for 2D UM materials.

Appendix D

Proposition: Given three non-zero symmetric second order tensors $\mathbf{S}_1$, $\mathbf{S}_2$ and $\mathbf{S}_3$, orthogonal to each other, such that they are of plane state with a common plane, then any three vectors defined by $\mathbf{t}_i = \mathbf{S}_i \cdot \mathbf{n}$ (i = 1, 2, 3) are always coplanar.

Demonstration: according to Appendix A, if the tensors $\mathbf{S}_i$ (i = 1, 2, 3) all are of plane states with a plane $\mathbf{m}$, the vectors $\mathbf{t}_i$ (i = 1, 2, 3) will always lie in such plane for any $\mathbf{n}$, i.e.,

$$\mathbf{S}_i \cdot \mathbf{m} = 0 \Rightarrow \forall \mathbf{n}, \mathbf{t}_i \cdot \mathbf{m} = 0, (i = 1, 2, 3)\,. \tag{D.1}$$

Since

$$rank\,([S_1, S_2, S_3]) \le 3, \tag{D.2}$$

where the tensor $\mathbf{S}$ is written in a vector form S with Voigt notation (same as those in Appendix C), the tensors $\mathbf{S}_1$, $\mathbf{S}_2$ and $\mathbf{S}_3$ mutually orthogonal each other require

$$rank\,([S_1, S_2, S_3]) = 3, \tag{D.3}$$

which is contained in the case of Eq. (D.2), so the proposition holds.

Without loss of generality, we can choose the following mutually orthogonal characteristic stresses which meet Eq. (D.3):

$$\begin{aligned} &\mathbf{S}_1 = \begin{bmatrix} S_{11}^{(1)} & 0 & 0 \\ 0 & 0 & 0 \\ 0 & 0 & 0 \end{bmatrix}, \mathbf{S}_2 = \begin{bmatrix} 0 & 0 & 0 \\ 0 & S_{22}^{(2)} & 0 \\ 0 & 0 & 0 \end{bmatrix}, \\ &\mathbf{S}_3 = \begin{bmatrix} 0 & S_{12}^{(3)} & 0 \\ S_{12}^{(3)} & 0 & 0 \\ 0 & 0 & 0 \end{bmatrix}. \end{aligned} \tag{D.4}$$

So, for the TM material, the three CFVs $\{\mathbf{t}_1, \mathbf{t}_2, \mathbf{t}_3\}$ can be coplanar for any $\mathbf{n}$, so the TM material can have only two slowness surfaces.

Corollary: when TM materials have three slowness surfaces, the innermost slowness surface is always closed, i.e., any three vectors defined by $\mathbf{t}_i = \mathbf{S}_i \cdot \mathbf{n}$ (i = 1, 2, 3) cannot be zero simultaneously.

Demonstration: if $\mathbf{t}_1$, $\mathbf{t}_2$ and $\mathbf{t}_3$ are equal to $\mathbf{0}$ with certain $\mathbf{n}^*$, then:

$$\mathbf{S}_1 \cdot \mathbf{n}^* = \mathbf{S}_2 \cdot \mathbf{n}^* = \mathbf{S}_3 \cdot \mathbf{n}^* = \mathbf{0}. \tag{D.5}$$

According to Appendix A, Eq. (D.5) indicates the tensors $\mathbf{S}_1$, $\mathbf{S}_2$ and $\mathbf{S}_3$ are of plane states with the plane $\mathbf{n}^*$. This would lead to Eq. (D.1), i.e., such TM materials have only two slowness surfaces, so the corollary holds.

Appendix E

Proposition: any four non-zero symmetric second order tensors $\mathbf{S}_i$ (i = 1, …, 4), mutually orthogonal to each other, they define four vectors $\mathbf{t}_i = \mathbf{S}_i \cdot \mathbf{n}$ (i = 1, …, 4). These four vectors cannot be always be coplanar.

Demonstration: if these four vectors are always coplanar within a plane $\mathbf{m}$, we would have:

$$\forall \mathbf{n}, \mathbf{t}_i \cdot \mathbf{m} \equiv 0, (i = 1, \ldots, 4)\,, \tag{E.1}$$

According to Appendix A, the following conditions can be obtained:

$$\mathbf{S}_i \cdot \mathbf{m} = \mathbf{0}, (i = 1, \ldots, 4)\,, \tag{E.2}$$

which indicates tensors $\mathbf{S}_i$ (i = 1,..,4) are of plane state with the plane $\mathbf{m}$, then:

$$rank\,([S_1, S_2, S_3, S_4]) \le 3, \tag{E.3}$$

where tensor **S** is written in a vector form S with Voigt notation as explained above. The Eq. (E.3) implies that the tensors $\mathbf{S}_i$ ($i = 1, \ldots, 4$) are no longer mutually orthogonal to each other, so the proposition holds.

Corollary: the innermost slowness surface of BM materials is always closed, i.e., any four vectors defined by $\mathbf{t}_i = \mathbf{S}_i \cdot \mathbf{n}$ ($i = 1, \ldots, 4$) cannot be zero simultaneously.

Demonstration: if $\mathbf{t}_i$ ($i = 1, \ldots, 4$) are equal to $\mathbf{0}$ with certain $\mathbf{n}^*$, then:

$$\mathbf{S}_1 \cdot \mathbf{n}^* = \mathbf{S}_2 \cdot \mathbf{n}^* = \mathbf{S}_3 \cdot \mathbf{n}^* = \mathbf{S}_4 \cdot \mathbf{n}^* = \mathbf{0}. \tag{E.4}$$

According to Appendix A, Eq. (E.4) implies that the tensors $\mathbf{S}_i$ ($i = 1,\ldots,4$) all are of plane states with the plane $\mathbf{n}^*$. While, this will lead to Eq. (E.3), implying that $\mathbf{S}_i$ ($i = 1, \ldots, 4$) are linearly dependent, so the corollary holds.

References

[1] D. Bigoni, D. Zaccaria, On the eigenvalues of the acoustic tensor in elastoplasticity, Eur. J. Mech. A Solids 13 (5) (1994) 621–638.

[2] N. Fang, D. Xi, J. Xu, M. Ambati, W. Srituravanich, C. Sun, X. Zhang, Ultrasonic metamaterials with negative modulus, Nature Mater. 5 (2006) 452–456.

[3] X.N. Liu, G.K. Hu, G.L. Huang, C.T. Sun, An elastic metamaterial with simultaneously negative mass density and bulk modulus, Appl. Phys. Lett. 98 (2011) 251907.

[4] R. Zhu, X.N. Liu, G.K. Hu, C.T. Sun, G.L. Huang, Negative refraction of elastic waves at the deep-subwavelength scale in a single-phase metamaterial, Nature Commun. 5 (2014) 5510.

[5] C. Scheibner, A. Souslov, D. Banerjee, P. Surówka, W.T.M. Irvine, V. Vitelli, Odd elasticity, Nat. Phys. 16 (4) (2020) 475–480.

[6] W. Cheng, G.K. Hu, Odd elasticity realized by piezoelectric material with linear feedback, Sci. China Phys. Mech. Astron. 64 (2021) 2.

[7] H. Nassar, Y.Y. Chen, G.L. Huang, A degenerate polar lattice for cloaking in full two-dimensional elastodynamics and statics, Proc. R. Soc. A 474 (2018) 20180523.

[8] H. Nassar, Y.Y. Chen, G.L. Huang, Isotropic polar solids for conformal transformation elasticity and cloaking, J. Mech. Phys. Solids 129 (2019) 229–243.

[9] H.K. Zhang, Y. Chen, X.N. Liu, G.K. Hu, An asymmetric elastic metamaterial model for elastic wave cloaking, J. Mech. Phys. Solids 135 (2020) 103796.

[10] G.W. Milton, A.V. Cherkaev, Which elasticity tensors are realizable? J. Eng. Mater. Technol. ASME 117 (1995) 483–493.

[11] G.W. Milton, The Theory of Composites, Cambridge University Press, Cambridge, United Kingdom, ISBN: 0-521-78125-6, 2002, xxviii + 719. (LCCNTA418.9. C6M58 2001).

[12] Y. Chen, X.N. Liu, G.K. Hu, Latticed pentamode acoustic cloak, Sci. Rep.-UK 5 (2015) 15745.

[13] C.N. Layman, C.J. Naify, T.P. Martin, D.C. Calvo, G.J. Orris, Highly anisotropic elements for acoustic pentamode application, Phys. Rev. Lett. 111 (2013) 024302.

[14] Y. Cheng, X.M. Zhou, G.K. Hu, Broadband dual-anisotropic solid metamaterials, Sci. Rep.-UK 7 (2017) 13197.

[15] M. Kadic, T. bückmann, R. Schittny, M. Wegener, On anisotropic versions of three-dimensional pentamode metamaterials, New J. Phys. 15 (2013) 023029.

[16] H.W. Dong, S.D. Zhao, X.B. Miao, C. Shen, X.D. Zhang, Z.G. Zhao, C.Z. Zhang, Y.S. Wang, L. Cheng, Customized broadband pentamode metamaterials by topology optimization, J. Mech. Phys. Solids 152 (2021) 104407.

[17] Z.Y. Li, Z. Luo, L.C. Zhang, C.H. Wang, Topological design of pentamode lattice metamaterials using a ground structure method, Mater. Des. 202 (2021) 109523.

[18] U.D. Larsen, O. Sigmund, S. Bouwstra, Design and fabrication of compliant micro-mechanisms and structures with negative Poisson's ratio, J. Microelectromech. Syst. 6 (1997) 99–106.

[19] J.N. Grima, K.E. Evans, Auxetic behavior from rotating squares, J. Mater. Sci. Lett. 19 (2000) 1563–1565.

[20] G.W. Milton, Adaptable nonlinear bimode metamaterials using rigid bars, pivots, and actuators, J. Mech. Phys. Solids 61 (7) (2013) 1561–1568.

[21] K. Wang, L.C. Wan, X.N. Liu, G.K. Hu, Precise design of unimode materials with periodic truss lattices, submitted.

[22] G.W. Milton, Complete characterization of the macroscopic deformations of periodic unimode metamaterials of rigid bars and pivots, J. Mech. Phys. Solids 61 (7) (2013) 1543–1560.

[23] Y. Wei, X.N. Liu, G.K. Hu, Quadramode materials: their design method and wave properties, Mater. Des. 210 (2021) 110031.

[24] M. Kadic, T. Bückmann, N. Stenger, M. Thiel, M. Wegener, On the practicability of pentamode mechanical metamaterials, Appl. Phys. Lett. 100 (19) (2012) 191901.

[25] R. Schittny, T. Bückmann, M. Kadic, M. Wegener, Elastic measurements on macroscopic three-dimensional pentamode metamaterials, Appl. Phys. Lett. 103 (23) (2013) 231905.

[26] A.N. Norris, Acoustic cloaking theory, Proc. R. Soc. Lond. Ser. A Math. Phys. Eng. Sci. 464 (2008) 2411–2434.

[27] T. Bückmann, M. Thiel, M. Kadic, R. Schittny, M. Wegener, An elastomechanical unfeelability cloak made of pentamode metamaterials, Nature Commun. 5 (2014) 4130.

[28] Y. Chen, M.Y. Zheng, X.N. Liu, Y.F. Bi, Z.Y. Sun, P. Xiang, J. Yang, G.K. Hu, Broadband solid cloak for underwater acoustics, Phys. Rev. B 95 (2017) 180104(R).

[29] M.Y. Zheng, C.I. Park, X.N. Liu, R. Zhu, G.K. Hu, Y.Y. Kim, Non-resonant metasurface for broadband elastic wave mode splitting, Appl. Phys. Lett. 116 (2020) 171903.

[30] J. Lee, M. Kweun, W. Lee, C.I. Park, Y.Y. Kim, Perfect transmission of elastic waves obliquely incident at solid–solid interfaces, Extreme Mech. Lett. 51 (2022) 101606.

[31] F. Fraternali, A. Amendola, Mechanical modeling of innovative metamaterials alternating pentamode lattices and confinement plates, J. Mech. Phys. Solids 99 (2017) 259–271.

[32] Y. Chen, B.H. Zhao, X.N. Liu, G.K. Hu, Highly anisotropic hexagonal lattice material for low frequency water sound insulation, Extreme Mech. Lett. 40 (2020) 100916.

[33] J.F. Yin, L. Cai, X. Fang, Y. Xiao, H.B. Yang, H.J. Zhang, J. Zhong, H.G. Zhao, D.L. Yu, J.H. Wen, Review on research progress of mechanical metamaterials and their applications on vibration and noise control, Adv. Mech. 52 (3) (2022) 1–79.

[34] Y. Chen, X.N. Liu, P. Xiang, G.K. Hu, Pentamode material for underwater acoustic wave control, Adv. Mech. 46 (2016) 201609.

[35] J.D. Achenbach, Wave Propagation in Elastic Solids, Elsevier, ISBN: 978-0-7204-0325-1, 1973.

[36] R. Hill, A general theory of uniqueness and stability in elastic–plastic solids, J. Mech. Phys. Solids 6 (3) (1958) 236–249.

[37] C.L. Chow, M. Jie, X. Wu, A damage-coupled criterion of localized necking based on acoustic tensor, Int. J. Damage Mech. 16 (3) (2007) 265–281.

[38] R. Bronson, G.B. Costa, J.T. Saccoman, Linear Algebra: Algorithms, Applications, and Techniques, Elsevier, ISBN: 978-0-12-391420-0, 2014.

[39] C.S. Jog, Continuum Mechanics: Foundations and Applications of Mechanics, Cambridge University Press, Cambridge, United Kingdom, ISBN: 9781316134054, 2015.